Available online at www.sciencedirect.com
SCIENCE DIRECT®
Journal of Sound and Vibration 275 (2004) 973–990
JOURNAL OF SOUND AND VIBRATION
www.elsevier.com/locate/jsvi

Stochastic optimal preview control of a vehicle suspension

Javad Marzbanrad[a,b], Goodarz Ahmadi[b,*], Hassan Zohoor[c], Yousef Hojjat[d]

[a] *Department of Automotive Engineering, Iran University of Science and Technology, Tehran, Iran*
[b] *Department of Mechanical and Aeronautical Engineering, Clarkson University, Camp Building, P.O. Box 5725, Potsdam, NY 13699-5725, USA*
[c] *Department of Mechanical Engineering, Sharif University of Technology, Tehran, Iran*
[d] *Department of Mechanical Engineering, Tarbiat Modarres University, Tehran, Iran*

Received 1 May 2001; accepted 3 July 2003

Abstract

Stochastic optimal control of a vehicle suspension on a random road is studied. The road roughness height is modelled as a filtered white noise stochastic process and a four-degree-of-freedom half-car model is used in the analysis. It is assumed that a sensor is mounted in the front bumper that measures the road irregularity at some distances in the front of the vehicle. Two other sensors also measure relative velocities of the vehicle body with respect to the unsprung masses in the vehicle suspension spaces. All measurements are assumed to be conducted in a noisy environment. The state variables of the vehicle system are estimated using a method similar to the Kalman filter. The suspension system is optimized by minimizing the performance index containing the mean-square values of body accelerations (including effects of heave and pitch), tire deflections and front and rear suspension rattle spaces. The effect of delay between front and rear wheels is included in the analysis. For stochastic active control with and without preview, the suspension performance and the power demand are evaluated and compared with those of the passive system. The results show that the inclusion of time delay between the front and rear axles and the preview information measured by the sensor mounted on the vehicle improves all aspects of the suspension performance, while reducing the energy consumption.

1. Introduction

Using active vibration control mechanisms for design of advanced suspension system has attracted considerable attention in recent years. The main concept is use an active suspension to

*Corresponding author. Tel.: +1-315-268-6586; fax: +1-315-268-6438.
E-mail addresses: marzban@iust.ac.ir (J. Marzbanrad), ahmadi@clarkson.edu (G. Ahmadi), zohoor@sharif.ac.ir (H. Zohoor).

0022-460X/$ - see front matter © 2003 Elsevier Ltd. All rights reserved.
doi:10.1016/S0022-460X(03)00812-5

reduce the vibration energy of the vehicle body induced by the road excitation, while keeping the vehicle stability within an acceptable limit.

While feedback control of vibrations has been extensively studied in the past, consideration of feed-forward (or preview) vibration control is relatively new. Preview active control of suspension involves the acquisition and use of information concerning the road profile ahead of the vehicle. Use of road preview information for improving vehicle suspension system was first proposed by Bender [1]. Tomizuka [2–4] described the implementation aspect of the preview control of suspension in practice. Thompson et al. [5], and Pilbeam and Sharp [6] used a state space approach and analyzed the suspension control for a quarter car model. Sasaki et al. [7], Iwata and Nakano [8], Foag and Grubel [9], Louam et al. [10], and Sharp and Wilson [11] considered a two-dimensional half-car model, which is supported by front and rear suspensions. Fruhauf et al. [12], Crolla and Abdel-Hadi [13], and Marzbanrad et al. [14,15], used a full-car configuration and analyzed the active control of suspension with the use of preview information. Morita [16] discussed the problems associated with the practical aspect of sensing the preview information. Hac et al. [17–19] proved that the front suspension performance improves by the use of the preview information in an active suspension system.

In preview active control of suspension, there are two sets of variables that need to be sensed and used in the control scheme. Preview of road irregularity information is used as the feed-forward component of the control strategy, while the state variables of the suspension system provide the basis for the feedback part of the control scheme. These variables need to be measured and be used in the implementation of the optimal control law. In practice, however, not all of the state variables can be measured. For the design of the control system, the variables that are not measured directly must be estimated. In addition, sensors commonly introduce noise during the measurement. In most previous studies on preview active control, it was assumed that all state variables are measured and the effect of the noisy environment was ignored. Thompson [20] also noted the difficulties associated with measuring all state variables in practical applications.

In the present study, active suspension control of a half-car model with and without preview is studied. The case that a sensor is mounted at the front bumper of the car that provides preview information concerning the road profile ahead of the vehicle is studied in detail. (Ultrasonic sensors are considered to be suitable for measuring the road unevenness ahead of the front bumper.) When the preview information is not available, the case that the active control system of the rear suspension has access to the information of front tire is analyzed. The suspension response results are compared with those of active system with no preview information and those of passive suspension.

The effect of noise in the measurement of state variables, and simultaneous wheel base delay preview are included in the analysis. Furthermore, it is assumed that only the vehicle body-unsprung mass relative velocities in the front and rear wheel suspension spaces are accessible for measurement. Therefore, the full state of the car is estimated using a method similar to the Kalman filter and Linear-Quadratic-Gaussian (LQG) controller. A third order filtered white noise model for the road roughness is used, and stochastic optimal controls with ride comfort and road holding preferences are then studied. For the ride comfort preference, the emphasis is placed on the comfort of passengers and on suppressing the vibration of sprung mass. Road holding preference, however, emphasizes the stability of the vehicle in following the road surface irregularities and more effectively minimizes the tire deflections.

2. Road profiles

Procedures for simulating road surface profiles that is consistent with the available measurements have been reported by Robson [21], Ruf [22], and Cebon and Newland [23]. In this paper, the road surface elevation power spectral density suggested by Rotenberg [24], which is applicable for a number of roads, is used. That is

$$S(\omega) = (\sigma_1^2/\pi)[\alpha_1 v/(\omega^2 + \alpha_1^2 v^2)] + (\sigma_2^2/\pi)[\alpha_2 v(\omega^2 + \alpha_2^2 v^2 + \beta^2 v^2)]/[(\omega^2 + \alpha_2^2 v^2 - \beta^2 v^2)^2 + 4\alpha_2^2 \beta^2 v^4], \quad (1)$$

where ω is the angular frequency, v is the vehicle velocity, $\alpha_1, \alpha_2, \beta, \sigma_1^2, \sigma_2^2$ are the coefficients depending on the type of road/train. The values of parameters for paved roads that are used in this study are listed in Table 1.

The time history of the road excitation corresponding to the spectral intensity given by Eq. (1) can be generated by passing a white noise process through a linear third order filter given as

$$\dddot{w} + (a_1 + a_3)\ddot{w} + (a_0 + a_1 a_3)\dot{w} + a_0 a_1 w = d_1(\ddot{\xi} + b_3\dot{\xi} + b_0\xi). \quad (2)$$

Here

$$\begin{aligned} a_0 &= -(\alpha_2^2 + \beta^2)v^2, \quad a_1 = \alpha_1 v, \\ a_2 &= 2(\alpha_2^2 - \beta^2)v^2, \quad a_3 = (a_2 + 2a_0)^{1/2}, \\ b_0 &= -[\sigma_1^2\alpha_1(\alpha_2^2 + \beta^2)^2 + \sigma_2^2\alpha_1^2\alpha_2(\alpha_2^2 + \beta^2)]^{1/2} v^{5/2}/b_4^{1/2}, \\ b_2 &= [2\sigma_1^2\alpha_1(\alpha_2^2 - \beta^2)^2 + \sigma_2^2\alpha_2(\alpha_1^2 + \alpha_2^2 + \beta^2)]v^3/b_4, \\ b_3 &= (b_2 + 2b_0)^{1/2}, \quad b_4 = (\sigma_1^2\alpha_1 + \sigma_2^2\alpha_2)v, \\ d_1 &= (b_4/\pi)^{1/2}. \end{aligned} \quad (3)$$

The filter Equation (2) may be presented in a matrix form as [25]

$$\dot{w} = F_w w + D_w \xi \quad (4)$$

with

$$F_w = \begin{bmatrix} 0 & 1 & 0 \\ 0 & 0 & 1 \\ -a_0 a_1 & -a_0 - a_1 a_3 & -a_1 - a_3 \end{bmatrix}, \quad D_w = \begin{bmatrix} d_1 \\ d_2 \\ d_3 \end{bmatrix}, \quad (5)$$

where

$$d_2 = d_1(b_3 - a_1 - a_3), \quad d_3 = d_1(b_0 - a_0 - a_1 a_3) - d_2(a_1 + a_3). \quad (6)$$

Table 1
Parameter values for spectrum of paved road

α_1 (m^{-1})	α_2 (m^{-1})	β (m^{-1})	σ_1^2 (m^2)	σ_2^2 (m^2)
0.5	0.2	2.0	2.55×10^{-4}	4.5×10^{-3}

In Eqs. (2) and (4), ξ, is a scalar white noise process. In this study, the intensity of ξ is selected so that the random road has a surface irregularity standard deviation of 0.01 m.

3. Suspension model

A half-car model as shown in Fig. 1 is used in the present stochastic optimal control study. The model has four degrees of freedom, including the vertical motions for unsprung masses of front and rear wheels and motions of the sprung mass including heave and pitch. Assuming the pitch motion is small, the equations of motion are given as

$$\begin{aligned} M\ddot{z}_c &= f_f + f_r, \\ I\ddot{\theta} &= f_f a + f_r b, \\ m_f\ddot{z}_1 &= -k_{f2}(z_1 - z_{01}) - f_f, \\ m_r\ddot{z}_2 &= -k_{r2}(z_2 - z_{02}) - f_r, \end{aligned} \tag{7}$$

where

$$\begin{aligned} f_f &= k_{f1}(z_1 - z_c - a\theta) + b(\dot{z}_1 - \dot{z}_c - a\dot{\theta}) + u_1, \\ f_r &= k_{r1}(z_2 - z_c + b\theta) + b(\dot{z}_2 - \dot{z}_c + b\dot{\theta}) + u_2. \end{aligned} \tag{8}$$

In these equations M and I are the sprung mass and its mass moment of inertia, m_f and m_r are the front and rear unsprung masses, respectively, and u_1 and u_2 are the control forces. Parameters k_{f1}, k_{r1} and b_f, b_r denote the stiffness and damping coefficient of passive suspension elements for front and rear assembles. Similarly, k_{f2} and k_{r2} denote the front and rear tire stiffness. Note that the tire damping which is much smaller than the damping of the suspension shock absorber is neglected.

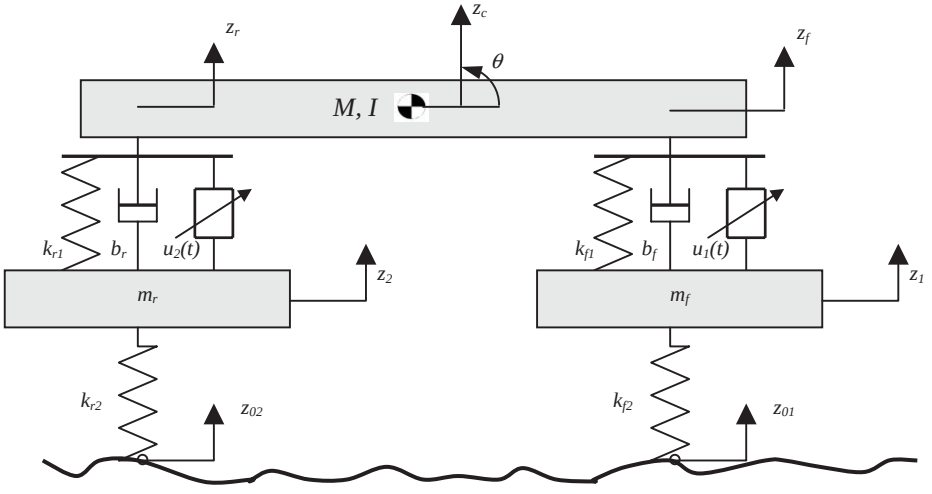

Fig. 1. Half-car suspension vehicle model.

Here it is assumed that the control actuation systems and the measuring instruments are mounted in the front and rear suspension spaces. Introducing the relative velocity

$$y_1(t) = \dot{z}_c + a\dot{\theta} - \dot{z}_1, \quad y_2(t) = \dot{z}_c - b\dot{\theta} - \dot{z}_2. \tag{9}$$

We define the state variable, x, the control input, u, the disturbance input, w, and the output y_0 as

$$x = [x_1, x_2, ..., x_8]^{\mathrm{T}}, \quad u = [u_1, u_2]^{\mathrm{T}}, \quad w = [w_1, w_2]^{\mathrm{T}}, \quad y_0 = [y_1, y_2]^{\mathrm{T}}, \tag{10}$$

where the state variable components are

$$\begin{aligned} x_1 &= z_c + a\theta - z_1, \quad x_2 = \dot{z}_c + a\dot{\theta}, \\ x_3 &= z_c - b\theta - z_2, \quad x_4 = \dot{z}_c - b\dot{\theta}, \\ x_5 &= z_1 - z_{01}, \quad x_6 = \dot{z}_1, \\ x_7 &= z_2 - z_{02}, \quad x_8 = \dot{z}_2. \end{aligned} \tag{11}$$

The components of the input disturbance (the rate of change in the height of road irregularities) for front and rear roads are

$$w_1(t) = \dot{z}_{01}(t), \quad w_2(t) = w_1(t - t_d). \tag{12}$$

where t_d represents the time delay between front and rear tire axis. Eqs. (7)–(9) may then be restated in the form of the state and output equations as

$$\dot{x}(t) = Ax(t) + Bu(t) + Dw(t), \tag{13}$$

$$y(t) = Cx(t) + v(t), \tag{14}$$

where A, B, D and C are constant matrices of dimension 8×8, 8×2, 8×2 and 2×8, respectively, that are given in Appendix A. In Eq. (14), $v(t) = [v_1(t), v_2(t)]^{\mathrm{T}}$ is the sensor measurement noise, which is assumed to be a vector white noise process.

The goal of the optimal design is to reduce a performance index subject to certain constraints. The design of vehicle suspension system normally involves a compromise among conflicting objectives. While achieving ride comfort amounts to reducing the accelerations of vehicle body, decreasing the dynamic tire forces are required for improving the road holding and stability of vehicles in facing the road irregularities. In practice, the control actuator forces have limitation and need to be reduced. These demands can be translated in finding the control-input u, which minimizes the quadratic performance index

$$\begin{aligned} J = \lim_{T\to\infty} \frac{1}{2T} \int_0^T E\Bigg\{ & \begin{bmatrix} \ddot{z}_c \\ \ddot{\theta} \end{bmatrix}^{\mathrm{T}} \begin{bmatrix} \rho_1 & 0 \\ 0 & \rho_2 \end{bmatrix} \begin{bmatrix} \ddot{z}_c \\ \ddot{\theta} \end{bmatrix} + \begin{bmatrix} x_1 \\ x_3 \end{bmatrix}^{\mathrm{T}} \begin{bmatrix} \rho_3 & 0 \\ 0 & \rho_4 \end{bmatrix} \begin{bmatrix} x_1 \\ x_3 \end{bmatrix} \\ & + \begin{bmatrix} x_5 \\ x_7 \end{bmatrix}^{\mathrm{T}} \begin{bmatrix} \rho_5 & 0 \\ 0 & \rho_6 \end{bmatrix} \begin{bmatrix} x_5 \\ x_7 \end{bmatrix} + \begin{bmatrix} u_1 \\ u_2 \end{bmatrix}^{\mathrm{T}} \begin{bmatrix} \rho_7 & 0 \\ 0 & \rho_8 \end{bmatrix} \begin{bmatrix} u_1 \\ u_2 \end{bmatrix} \Bigg\} \mathrm{d}t. \end{aligned} \tag{15}$$

The weighting constants, $\rho_i, i = 1, ..., 8$, reflect the designer preferences in balancing different effects in the performance index given by Eq. (15). After substituting for the acceleration $\ddot{z}_c$ and $\ddot{\theta}$ from Eq. (7) and using Eqs. (11) and (12), the performance index may be expressed in quadratic

form as

$$J = \lim_{T\to\infty} \frac{1}{2T} \int_0^T E(x^{\mathrm{T}} Q_1 x + 2x^{\mathrm{T}} N u + u^{\mathrm{T}} R u + 2x^{\mathrm{T}} Q_{12} w + w^{\mathrm{T}} Q_2 w)\, \mathrm{d}t, \tag{16}$$

where Q_1, N, R, Q_{12} and Q_2 are time-invariant, symmetric weighting matrices subject to the condition that $Q_n = Q_1 - R^{-1}N^{\mathrm{T}}$ is a positive semi-definite matrix.

4. Optimal preview control formulation

In this section the formulation of the optimal preview control problem is described. The formulation takes into account the fact that only a limited number of the state variables can be measured with sensors. It is also assumed that the preview information about the road roughness $w(\tau)$ up to t_p time units ahead of t, is available. In general, however, the available measurements of the state variables are noisy, as are the measurements of the road surface profile ahead of time. Measurement noise usually represents a random disturbance with zero mean and short correlation times compared to the characteristic time constants of the system. Therefore, the measurement noise is normally modelled as a white noise process.

Fundamentals of deterministic and stochastic linear optimal preview control problems were described in Ref. [17]. The main results may be summarized in the following theorem.

Theorem 1. *Given a system with state equation* (13) *and with preview time*, t_P, *that is with* $w(\sigma), \sigma \in [t + t_P]$ *known, the problem is to find a control law* $u(t) = f(x(t), w(\sigma), \sigma \in [t + t_p])$ *that minimizes the quadratic performance index given by* Eq. (16).

Introducing the notation

$$A_n = A - BR^{-1}N^{\mathrm{T}}, \quad Q_n = Q_1 - NR^{-1}N^{\mathrm{T}} \tag{17}$$

and assuming that Q_n is non-negative definite and factoring Q_n such that $Q_n = T^{\mathrm{T}}T$, then if the pair (A_n, B) is stabilizable and the pair (A_n, T) is detectable, the optimal preview control force is given by

$$u_0(t) = K_1 x(t) + K_2 r(t), \quad K_1 = -R^{-1}(N^{\mathrm{T}} + B^{\mathrm{T}}P), \quad K_2 = -R^{-1}B^{\mathrm{T}}, \tag{18}$$

where P is the positive definite solution of the Algebraic Riccati equation

$$PA_n + A_n^{\mathrm{T}}P - PBR^{-1}B^{\mathrm{T}}P + Q_n = 0. \tag{19}$$

In Eq. (18), the vector $r(t)$ is given by

$$r(t) = \int_0^{t_p+t_d} \mathrm{e}^{A_c^{\mathrm{T}}\sigma}(PD + Q_{12}) \begin{bmatrix} H(t_p - \sigma) w_1(t + \sigma) \\ w_1(t + \sigma - t_d) \end{bmatrix} \mathrm{d}\sigma, \tag{20}$$

where

$$\mathrm{H}(t_p - \sigma) = \begin{cases} 1 & \text{for } \sigma \leqslant t_p \\ 0 & \text{for } \sigma > t_p \end{cases} \tag{21}$$

is the Heaviside (unit step) function, t_d is the time delay for second input with respect to the first input, and matrix A_c is given by

$$A_c = A - BR^{-1}(N^{\mathrm{T}} + B^{\mathrm{T}}P) = A_n - BR^{-1}B^{\mathrm{T}}P. \tag{22}$$

It should be emphasized that A_c is the closed-loop system matrix, which is asymptotically stable, and therefore has eigenvalues with negative real parts.

Theorem 2. *Consider a system with state space equations* (13) and (14), *the preview time and cost function as given in* Theorem 1, *and the observed input variable* $w^*(t)$ *given by*

$$w^*(t) = w(t + t_p) + \eta(t) \tag{23}$$

with $col(\eta, v)$ *being a zero mean stationary vector white noise process with autocorrelation*

$$E\left\{ \begin{bmatrix} \eta(t) \\ v(t) \end{bmatrix} \begin{bmatrix} \eta^{\mathrm{T}}(\tau) & v^{\mathrm{T}}(\tau) \end{bmatrix} \right\} = \begin{bmatrix} V_1 & 0 \\ 0 & V_2 \end{bmatrix} \delta(t - \tau), \tag{24}$$

where $V_1 > 0$ *and* $V_2 > 0$ *are the noise intensities, and the initial state* x_0 *is uncorrelated with* w, v *and* η. *Then the optimal preview control force is given by*

$$u_0(t) = K_1\hat{x}(t) + K_2\hat{r}(t); \quad K_1 = -R^{-1}(N^{\mathrm{T}} + B^{\mathrm{T}}P), \quad K_2 = -R^{-1}B^{\mathrm{T}}, \tag{25}$$

where $\hat{x}(t)$ *and* $\hat{r}(t)$ *are estimated parameters given by*

$$\dot{\hat{x}} = A\hat{x}(t) + Bu(t) + L(t)[y(t) - C(t)\hat{x}(t)] + Dw^*(t - t_p), \tag{26}$$

$$\dot{\hat{r}} = (-A_n^{\mathrm{T}} + PBR^{-1}B^{\mathrm{T}})\hat{r} - (PD + Q_{12})w^*(t - t_p) \tag{27}$$

with P defined by Eq. (19). *Here L is the solution of optimal observer problem and given by*

$$L(t) = S(t)C^{\mathrm{T}}V_2^{-1}, \tag{28}$$

where S is the solution of Algebraic Riccati equation

$$AS + SA^{\mathrm{T}} - SC^{\mathrm{T}}V_2^{-1}CS + V_1 = 0. \tag{29}$$

As pointed out by Hac [17] *the observer structure is similar to that of the classical Kalman–Bucy filter, with the only new feature being the presence of the term* $Dw^*(t - t_p)$ *in* Eq. (26), *which is an estimate of* $Dw(t - t_p)$.

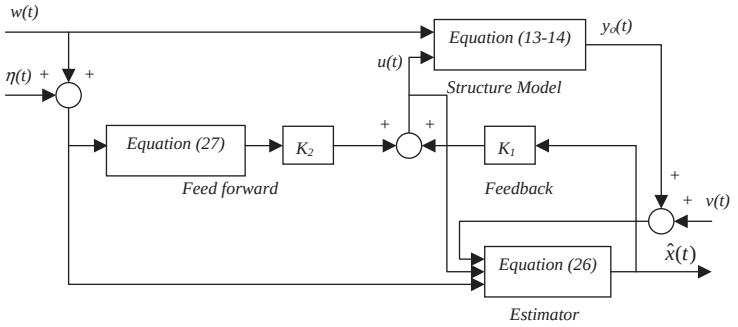

Fig. 2. Block diagram for control system with feedback, feed-forward and estimator.

Fig. 2 illustrates a block diagram of the stochastic active preview system based on Theorems 1 and 2. This diagram shows the feedback, feed-forward and estimator terms and together with measurement noises that comes with measuring the road input and suspension space parameters. When preview is not available, the feedback term remains and the control scheme reduces to the classical LQG theory for active suspension.

It should be emphasized that the dynamical system for the filtered white noise model of the road input through Eq. (4) is combined with the vehicle system dynamics given by Eqs. (13) and (14) to obtain an augmented over all system dynamics given by

$$\dot{x}_s = A_s x_s + B_s u + D_s \xi, \tag{30}$$

$$y_s = C_s x_s + v, \tag{31}$$

where

$$x_s = \begin{bmatrix} x \\ w \end{bmatrix}, \quad A_s = \begin{bmatrix} A & D \\ 0 & F_w \end{bmatrix}, \quad B_s = \begin{bmatrix} B \\ 0 \end{bmatrix}, \quad D_s = \begin{bmatrix} 0 \\ D_w \end{bmatrix}, \quad C_s = \begin{bmatrix} C & 0 \end{bmatrix}. \tag{32}$$

The augmented system now has a scalar white process noise $\xi(t)$ as input; therefore, the response x_s is a vector Markov process.

5. Numerical simulation

In this section, the results concerning the stochastic optimal control of a half-car suspension model with and without preview sensors on a random road are studied. The performance of active systems with and without preview are compared with that of the passive system. Effects of noisy environment on the sensor measurements are also included in the analysis. It is assumed that one sensor is mounted on the front bumper that measures the road unevenness ahead of the front tire. Two other sensors measure the relative velocities in suspension spaces, y_1, y_2 of the front and the rear tires. The LQG method is utilized for estimating state variables as shown in the block diagram in Fig. 2. The vehicle parameters for a compact sedan that are used in simulation are listed in Table 2. Two sets of weighting constants in the performance index given by Eq. (15) for the ride comfort and the road holding are used in the study. The corresponding weighting constants together with the closed-loop system poles are listed in Table 3.

Table 2
Vehicle model parameter values

Parameter	Value	Parameter	Value
M	500 kg	I	910 kg m^2
m_1	30 kg	m_2	40 kg
a	1.25 m	b	1.45 m
k_{f1}	10 000 N/m	k_{r1}	10 000 N/m
k_{f2}	100 000 N/m	k_{r2}	100 000 N/m
b_f	1000 N s/m	b_r	1000 N s/m

Table 3
Weighting constants for both design and the corresponding closed-loop system poles

Ride comfort			Road holding		
Weighting constants		Eigenvalues	Weighting constants		Eigenvalues
1	1	−8.43 + 58.3i	1	1	−20.40 + 61.14i
2	2	−8.43−58.3i	2	2	−20.40−61.145i
3	1100	−6.76 + 50.4i	3	3200	−15.02 + 52.1i
4	1200	−6.76−50.4i	4	3300	−15.02−52.1i
5	5600	−4.33 + 4.86i	5	40000	−5.01 + 5.94i
6	5500	−4.33−4.86i	6	32000	−5.01−5.94i
7	1e−8	−4.62 + 5.18i	7	1e−8	−5.39 + 6.40i
8	1e−8	−4.62−5.18i	8	1e−8	−5.39−6.40i

5.1. Vehicle response

Vehicle vertical and angular acceleration time histories for different suspension control systems are shown in Fig. 3. The cases of passive, active, active and delay, and active and preview suspension are shown. In the case of active and delay, it is assumed that the rear tire control uses the information of the front tire, but the front tire does not have any preview information of the road condition. In the case of active and preview control, however, the front tire uses the information of sensor that measures the road irregularities ahead of the car. The active control corresponds to the case with no preview information for front or rear tire. Unless stated otherwise, a preview time of 0.12 s for a vehicle with a velocity of 20 m/s is used in the analysis, and the simulation results are presented for 1.2 s. Fig. 3a and b show the results for the ride comfort preference, while the road holding preference results are shown in Fig 3c and d. As expected both vertical and angular accelerations for the ride comfort preference are lower than those for the road holding preference in all three cases of active systems. Fig. 3 shows that the vehicle accelerations for the cases with the preview control are lower than those with active especially with respect to passive system.

The small amplitude fluctuations seen in Fig. 3 are consequence of the road surface roughness. The passive suspension appears to filter out these high frequency contents of the road excitation. They however seem to persist for the active suspensions.

To provide insight into the nature of preview suspension control, the Fourier spectra of vertical and angular accelerations for passive and active systems are shown in Fig. 4. Frequency contents of acceleration response may be clearly seen from this figure. It is observed that the active control decreases the amplitudes of accelerations more effectively for the ride comfort preference.

Fig. 5 show the wheel tracking of suspension system (z_i) for passive and active suspensions. The corresponding road surface profiles are also shown by dash lines in this figure for comparison. This figure clearly shows that the front wheel actuator reacts before rear wheel. Also, for the suspension with preview control, the front wheel begins to respond to road irregularities sooner than is the case for active and delay or active system. It is also observed that the wheel tracking essentially follows the road unevenness. For road holding preference shown in Fig. 5c and d, however, the wheels follow the road much closer than the case for ride comfort preference shown

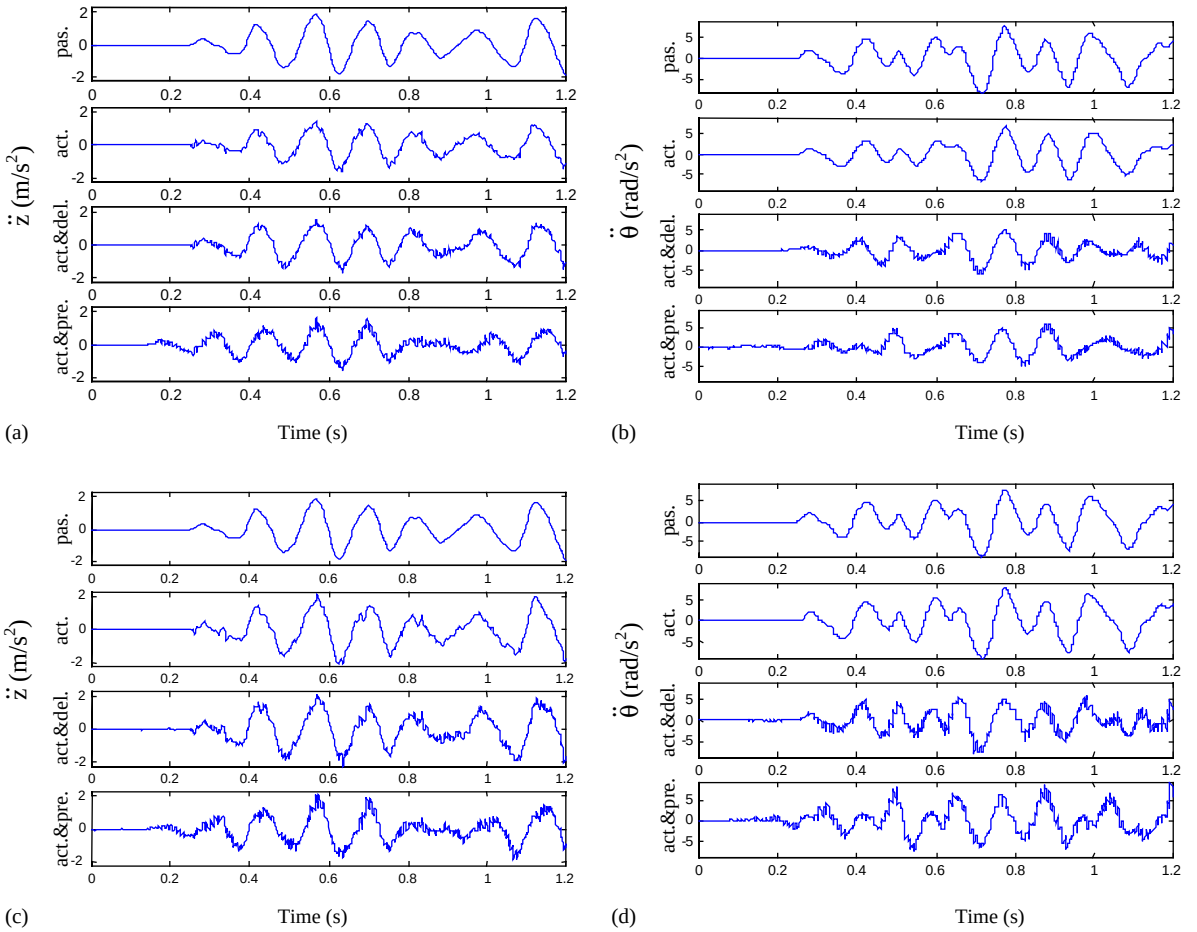

Fig. 3. Time histories of accelerations: (a) Vertical acceleration with ride comfort, (b) angular acceleration with ride comfort, (c) vertical acceleration with road holding, and (d) angular acceleration with road holding.

in Fig. 5a and b. Comparing the road tracking of preview active control with active control for both ride comfort and road holding preferences, it is seen that the preview control are closer to the road profile. Consequently, the preview control will provide better road holding for the vehicle. Fig. 5 also shows the presence of high frequency fluctuation for active control systems, which are caused by the noise environments for measuring suspension spaces and the road profile.

5.2. Power consumption

The power dissipated is given as

$$P_1 = F_1(\dot{z}_c + a\dot{\theta} - \dot{z}_1),$$
$$P_2 = F_2(\dot{z}_c + a\dot{\theta} - \dot{z}_2), \tag{33}$$

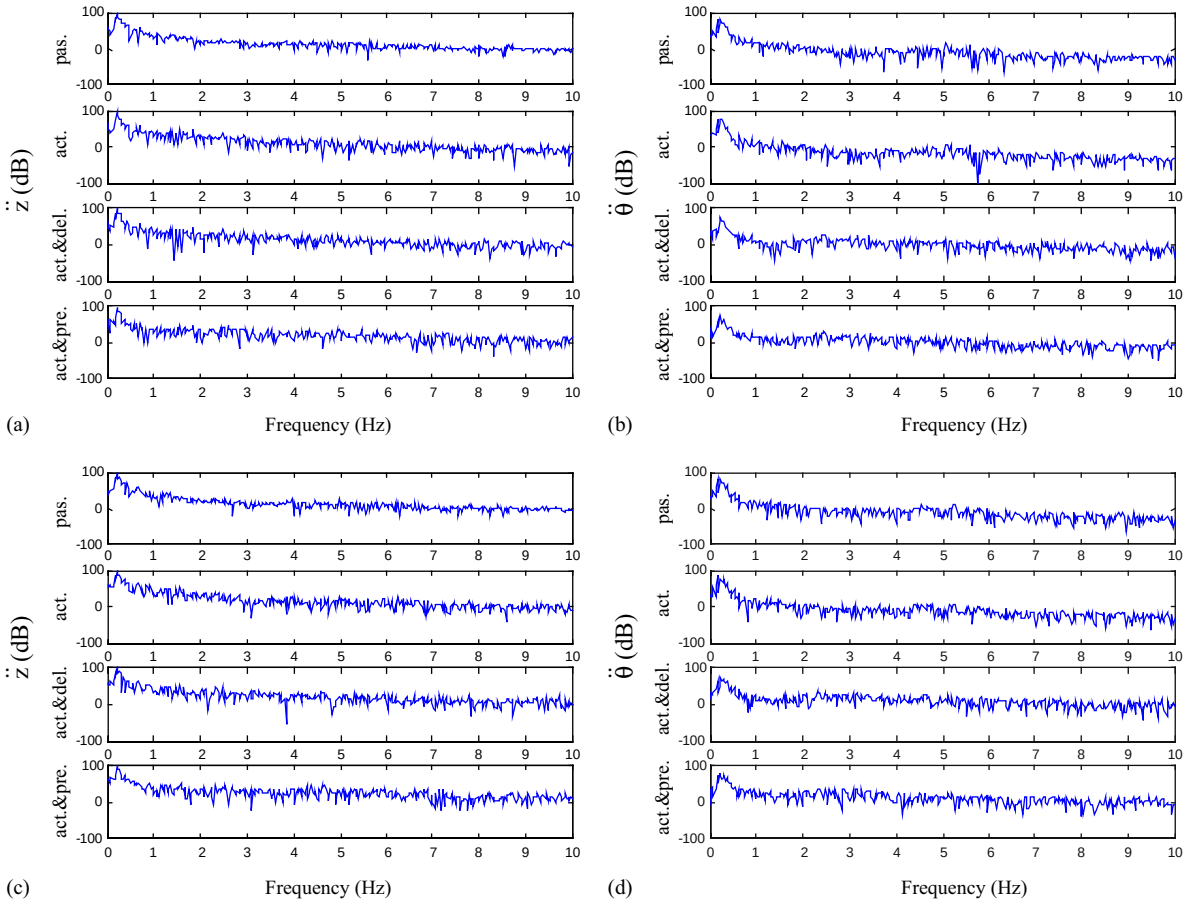

Fig. 4. Spectra of accelerations: (a) Vertical acceleration with ride comfort, (b) angular acceleration with ride comfort, (c) vertical acceleration with road holding, and (d) angular acceleration with road holding.

where F_1 and F_2 are force control together with the force that is dissipated by the damper, they are

$$F_1 = [b_f(\dot{z}_1 - \dot{z}_c - a\dot{\theta}) + u_1],$$
$$F_2 = [b_r(\dot{z}_2 - \dot{z}_c + b\dot{\theta}) + u_2]. \tag{34}$$

Fig. 6 shows time histories of power demand for the front and the rear wheels for both ride comfort and road holding preferences. It is noticed that there is no significant difference in the power consumption between the two preferences. The ride comfort preference, however, needs slightly less power than the road holding. Fig. 6 also shows that the power consumption for preview control is less than those for active and delay, and active system. The system without preview reacts only after the tire reaches the road irregularities, while the system with preview begins to reacts when receiving the preview information from the sensors.

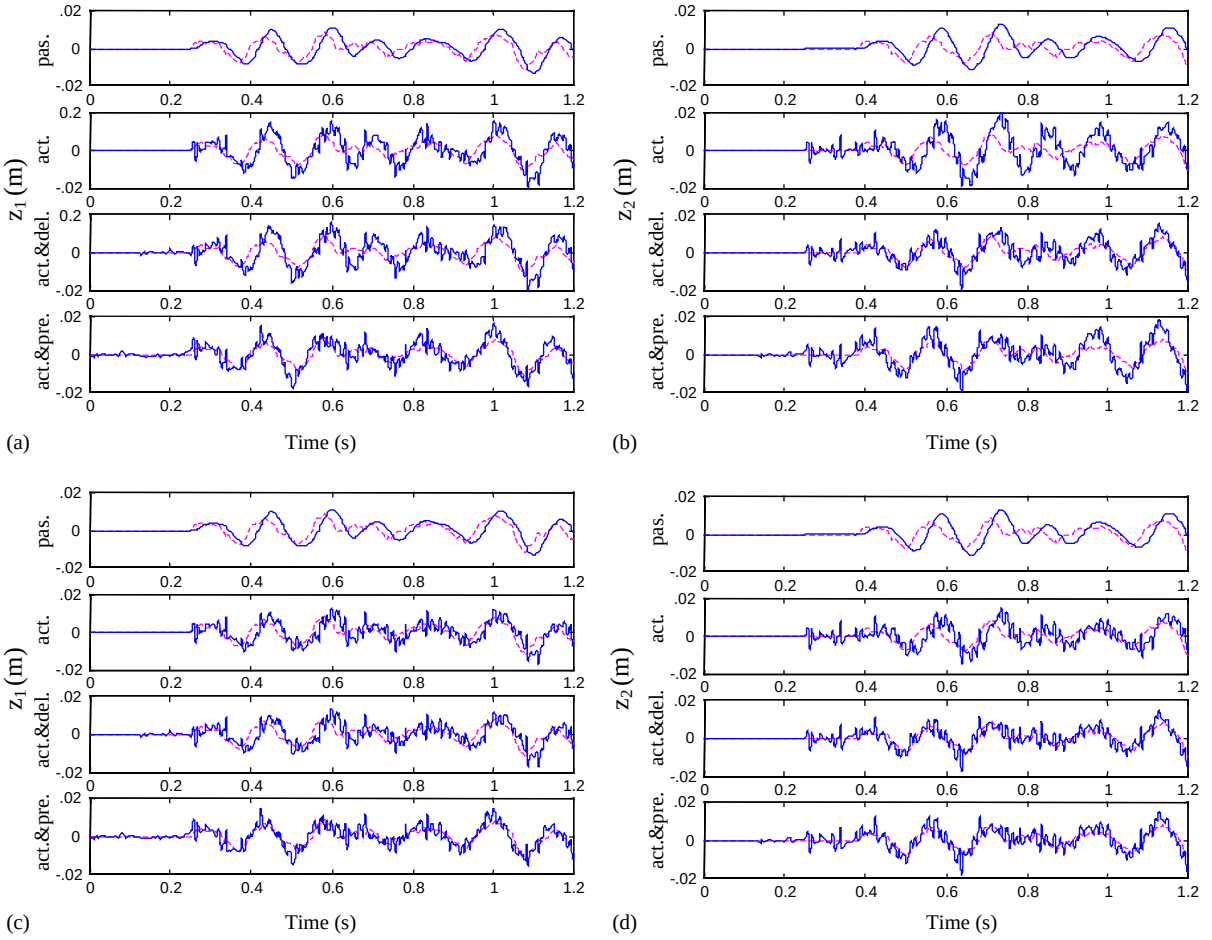

Fig. 5. Time histories of wheel tracking: (a) Front wheel with ride comfort, (b) rear wheel with ride comfort, (c) front wheel with road holding, and (d) rear wheel with road holding.

5.3. Mean-square values

The performance index J given by Eq. (15) contains accelerations, suspension rattle spaces, tire deflections, and control forces. Although the goal of optimization is to minimize the performance index, J, which is the summation of mean squares of these parameters, it is of interest to study the values of each of these parameters separately. Therefore, performance index and its corresponding parameters are evaluated for both preferences and the results are shown in Tables 4 and 5. Comparisons of results of estimated states are also performed in the case that full state-variables are available. For the full state-variable case, it is assumed that all states of Eq. (11) are measured precisely (with no noise). For the estimated state method, it is assumed that only the relative velocities in the suspension spaces as given by Eq. (9) are measurable with noisy sensors. In Tables 4 and 5, all values are normalized with respect to the corresponding values obtained for

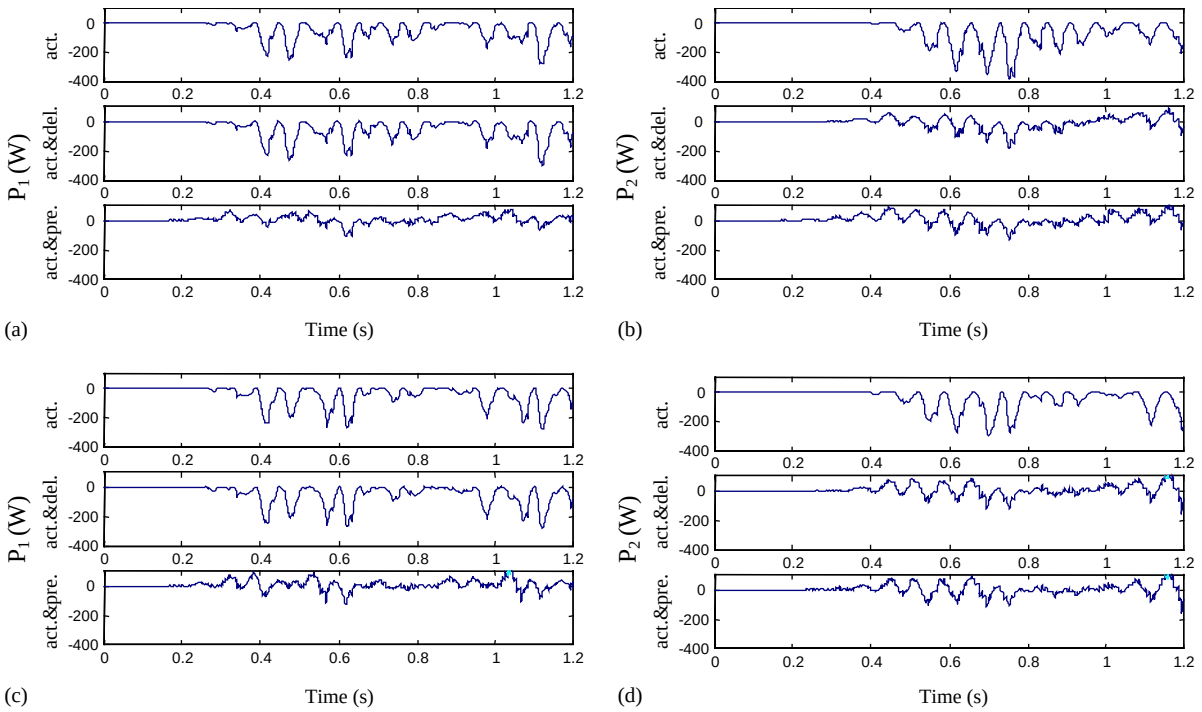

Fig. 6. Time histories of power demand: (a) Front wheel with ride comfort, (b) rear wheel with ride comfort, (c) front wheel with road holding, and (d) rear wheel with road holding

Table 4
Components of performance index with considering the passive system corresponds to 100 percent in ride comfort preference for full state (FS) and estimated method (EM)

System	$E(\ddot{z}_c^2)$		$E(\ddot{\theta}^2)$		$E(x_1^2)$		$E(x_3^2)$		$E(x_5^2)$		$E(x_7^2)$		J	
	FS	EM	FS	EM	FS	EM	FS	EM	FS	EM	FS	EM	FS	EM
Passive	100	100	100	100	100	100	100	100	100	100	100	100	**100**	**100**
Active	57.6	58.3	66.0	67.0	160.5	161.1	196.6	191.3	141.5	130.9	176.4	166.2	**83.8**	**82.5**
Active & delay	69.6	71.8	32.1	33.1	158.8	163.2	113.3	111.8	139.7	141.9	44.2	46.3	**68.5**	**70.3**
Active & preview	51.8	54.9	33.7	34.9	121.5	120.9	164.7	158.9	49.3	62.2	69.8	77.8	**54.7**	**58.4**

the passive system and are given as percentages. Here it is assumed that the preview time is 0.12 s and the paved road with the spectral intensity given by Eq. (1) is used.

Tables 4 and 5 show that the estimated method has values close to the full state approach. That is, the estimated method evaluates the states properly, and leads to results that are approximately the same as those obtained for the full state case, while requiring fewer state variable measurements. Tables 4 and 5 also show that the response accelerations for the ride comfort

Table 5
Components of performance index with considering the passive system corresponds to 100 percent in road holding preference for full state (FS) and estimated method (EM)

System	$E(\ddot{z}_c^2)$		$E(\ddot{\theta}^2)$		$E(x_1^2)$		$E(x_3^2)$		$E(x_5^2)$		$E(x_7^2)$		J	
	FS	EM	FS	EM	FS	EM	FS	EM	FS	EM	FS	EM	FS	EM
Passive	100	100	100	100	100	100	100	100	100	100	100	100	**100**	**100**
Active	100.3	104	110.0	111.0	87.6	89.5	88.6	87.4	80.2	76.1	81.4	79.8	**89.7**	**89.4**
Active & delay	121.5	125	52.7	54.3	87.7	92.2	80.3	80.4	80.4	87.7	15.5	22.0	**71.0**	**76.1**
Active & preview	90.7	92.9	91.4	94.3	89.0	88.8	95.3	92.2	19.3	36.3	19.0	31.2	**51.8**	**60.5**

preference are more effectively decreased when compared with those for the road holding preference. Similarly when the emphasis is on road holding, the tire deflections are more effectively reduced. However, the total amount of performance index for both ride comfort and road holding preference remains close to each other.

The results presented in Tables 4 and 5 show that the active and preview control leads to the lowest value of performance index among the different approaches for suspension control studied. Active and preview control not only decreases the performance index, J, but almost all mean-square responses as well. Active and delay control approach shows better performance with respect to the active control for suspension space and tire deflection of the rear tire. Incorporation of the time delay (between the front and rear wheel) reduces the angular acceleration more than twice with respect to the vertical acceleration, while active control shows about the same fraction for both accelerations. In summary, the performance index and different mean-square responses improve for all types of active system with the amount of improvement increasing as the control system becomes more complex from active, to active and delay, and to active and preview, respectively.

5.4. *Effect of preview time*

Vehicles moving with different velocities lead to variation of preview time. If the sensor that is mounted in the front bumper could see 2.4 m ahead, the preview time is 0.12 s for the vehicle velocity of 20 m/s (72 km/h). To study the effect of preview time, mean-square response of performance index and certain mean-square parameters for a range of preview times from 0.01 to 0.19 s for both ride comfort and road holding preference are evaluated and the results are shown in Fig. 7. In this Figure, the relative performance is defined as the ratio of responses in the case of active and preview control to the corresponding value of active control without preview (i.e., $t_p = 0$). Fig. 7 shows that the performance index, J, reaches a smooth value after about 0.1 s for ride comfort preference and after 0.04 s for road holding preference. This is because eigenvalues of the closed loop matrixA_c for the road holding preference have larger negative real parts when compared with the ride comfort case as shown in Table 3. It is also observed that additional increase in the preview time does not produce significant improvement in the performance index.

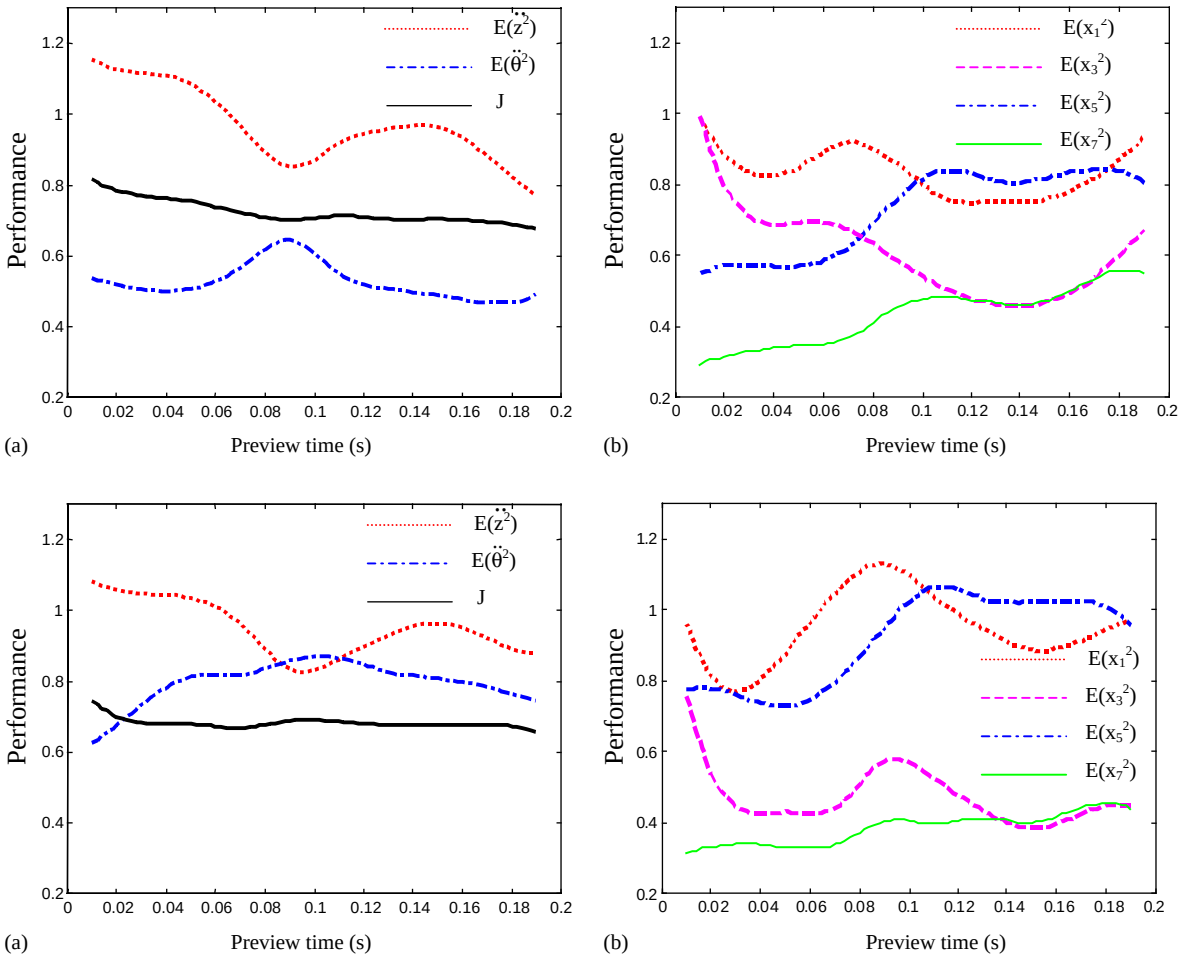

Fig. 7. Sensitive analysis of performance with respect to change of preview time: (a) Accelerations and total performance index with ride comfort, (b) suspension space and tire deflection performance with ride comfort, (c) accelerations and total performance index with road holding, and (d) suspension space and tire deflection performance with road holding.

Mean-square performance of angular acceleration is also presented in Fig. 7a and c. Angular acceleration shows an opposite trend of behavior to vertical acceleration for both preferences, although both performances improve for preview control. Fig. 7b and d show the performance with regard to the suspension space, and tire deflection for ride comfort and road holding, respectively. These figures show that the mean-square deflections of the rear wheel are less than those for the front wheel. This is because the rear wheel actuators have access to the information in a longer time interval. Fig. 7 essentially shows that good suspension design requires a compromise between various conflicting parameters for both ride comfort for passengers and road holding.

6. Conclusions

Responses of a vehicle suspension with active, active and delay, and active and preview control systems to random road input are evaluated and the results are compared with those for the passive system. Road surface elevation information at distance ahead of the bumper is used as preview and the suspension space velocities are measured by sensors in a noisy environment. Stochastic optimal control theory is used and the states are estimated by an observer, similar to a Kalman filter. On the basis of the results presented, the following conclusions are drawn:

1. The present results substantiate the earlier findings that properly designed optimal active suspensions with preview are highly effective in reducing the performance index and the mean-square responses during the vehicle travel on a random road.
2. The acceleration responses for optimal preview control are much lower in the ride comfort preference when compared with road holding case. The mean-square suspension spaces and tire deflections for road holding preference, however, are lower than those for the ride comfort case.
3. Mean-square responses of the suspension system decreases as the time delay and preview are added to control system.
4. Using the proposed state estimation method reduces the required measuring, while the results for optimized performance remain approximately the same.
5. A rather short time preview information of the road input is sufficient for improving the performance of the control system.
6. The performance of control system improves with an increase in the preview time up to a certain value. Further increase in the preview time does not produce significant improvement. However, the performance index of road holding preference reaches its optimum value sooner than ride comfort preference.
7. Magnitude of the control power consumption for active and preview control is less than active control system without preview.

It is recognized that the actuator dynamics affects the active control system performance with or without the preview. In this manuscript we have shown that the preview information improves the control system performance. One advantage of the preview control approach is that it can compensate for the time delays in the reactions of the system and the actuators; however, interactions of the actuation system with the suspension are not considered. Including these important coupling effects is left for a future communication.

Acknowledgements

The authors would like to thank Dr. James Carroll of Clarkson University for many helpful discussions.

Appendix A

System matrices are:

$$A = \begin{bmatrix} 0 & 1 & 0 & 0 & 0 & -1 & 0 & 0 \\ -k_{f1}a_1 & -b_f a_1 & -k_{r1}a_2 & -b_r a_2 & 0 & b_f a_1 & 0 & b_r a_2 \\ 0 & 0 & 0 & 1 & 0 & 0 & 0 & -1 \\ -k_{f1}a_2 & -b_f a_2 & -k_{r1}a_3 & -b_r a_3 & 0 & b_f a_2 & 0 & b_r a_2 \\ 0 & 0 & 0 & 0 & 0 & 1 & 0 & 0 \\ k_{f1}/m_1 & b_f/m_1 & 0 & 0 & -k_{f2}/m_1 & -b_f/m_1 & 0 & 0 \\ 0 & 0 & 0 & 0 & 0 & 0 & 0 & 1 \\ 0 & 0 & k_{r1}/m_2 & b_r/m_2 & 0 & 0 & -k_{r2}/m_2 & -b_r/m_2 \end{bmatrix},$$

$$B = \begin{bmatrix} 0 & 0 \\ a_1 & a_2 \\ 0 & 0 \\ a_2 & a_3 \\ 0 & 0 \\ -1/m_1 & 0 \\ 0 & 0 \\ 0 & -1/m_2 \end{bmatrix}, \quad D = \begin{bmatrix} 0 & 0 \\ 0 & 0 \\ 0 & 0 \\ 0 & 0 \\ -1 & 0 \\ 0 & 0 \\ 0 & -1 \\ 0 & 0 \end{bmatrix}, \quad C = \begin{bmatrix} 0 & 1 & 0 & 0 & 0 & -1 & 0 & 0 \\ 0 & 0 & 0 & 1 & 0 & 0 & 0 & -1 \end{bmatrix},$$

where

$$a_1 = 1/M + a^2/I, \quad a_2 = 1/M - ab/I, \quad a_3 = 1/M + b^2/I.$$

References

[1] E.K. Bender, Optimum linear preview control with application to vehicle suspension. American Society of Mechanical Engineers, *Journal of Basic Engineering* 100 (1968) 213–221.

[2] M. Tomizuka, The Optimal Finite Preview Problem and its Application to Man-Machine Systems, PhD Thesis, Massachusetts Institute of Technology, 1974.

[3] M. Tomizuka, Optimal continuos finite preview problem, *IEEE Transaction on Automatic Control* 20 (1975) 362–365.

[4] M. Tomizuka, Optimal linear preview control with application to vehicle suspension-revisited, *American Society of Mechanical Engineers, Journal of Dynamic Systems Measurement Control* 98 (3) (1976) 309–315.

[5] A.G. Thompson, B.R. Davis, C.E.M. Pearce, An optimal linear active suspension with finite road preview, SAE Transaction, Pennsylvania, paper 800520, 1980, pp. 2009–2020.

[6] C. Pilbeam, R.S. Sharp, Performance potential and power consumption of slow-active suspension systems with preview, *Vehicle System Dynamics* 25 (3) (1996) 169–183.

[7] M. Sasaki, J. Kamiya, T. Shimogo, Optimal preview control of vehicle suspension, *Bulletin of the Japan Society of Mechanical Engineers* 19 (129) (1976) 265–273.

[8] Y. Iwata, M. Nakano, Optimal preview control of vehicle air suspension, *Bulletin of the Japan Society of Mechanical Engineers* 19 (138) (1976) 1485–1489.
[9] Q. Foag, G. Grubel, Multi-criteria control design for preview vehicle suspension systems, *World Congress on Automatic Control*, 1987, pp. 189–195.
[10] N. Louam, D.A. Wilson, R.S. Sharp, Optimization and performance enhancement of active suspensions for automobiles under preview of the road, *Vehicle System Dynamics* 21 (1) (1992) 39–63.
[11] R.S. Sharp, D.A. Wilson, On control laws for vehicle suspensions accounting for input correlations, *Vehicle System Dynamics* 19 (6) (1990) 353–364.
[12] F. Fruhauf, R. Kasper, J. Luckel, Design of an active suspension for a passenger vehicle model using input processes with time delays, in: O. Nordström (Ed.), *Dynamics of Vehicles on Roads and Tracks*, Swets and Zeitlinger, Lisse, 1986, pp. 126–138.
[13] D.A. Crolla, M.B.A. Abdel-Hady, Active suspension control: performance comparisons using control laws applied to a full vehicle model, *Vehicle System Dynamics* 20 (2) (1991) 107–120.
[14] J. Marzbanrad, Y. Hojjat, H. Zohoor, S.K. Nikravesh, Optimal preview control design of an active suspension based on a full car model, *Scientia Iranica* 10 (2003) 23–36.
[15] J. Marzbanrad, G. Ahmadi, Y. Hojjat, H. Zohoor, Optimal active control of vehicle suspension systems including time delay and preview for rough roads, *Journal of Vibration and Control* 8 (2002) 967–991.
[16] T. Morita, T. Tanaka, N. Kishimoto, Riding comfort improvement using the preview sensors, *Proceeding AVEC'92*, SAE, Japan, 1992, pp. 111–116.
[17] A. Hac, Optimal linear preview control of active vehicle suspension, *Vehicle System Dynamics* 21 (3) (1992) 167–195.
[18] A. Hac, I. Youn, Optimal semi-active suspension with preview based on a quarter car model, *Transaction of the American Society of Mechanical Engineers, Journal of Vibration and Acoustics Stress and Reliability in Design* 114 (1) (1992) 84–92.
[19] A. Hac, I. Youn, Optimal design of active and semi-active suspensions including time delays and preview, *Transaction of the American Society of Mechanical Engineers, Journal of Vibration and Acoustics* 115 (1993) 498–508.
[20] A.G. Thompson, Optimal and suboptimal linear active suspensions for road vehicles, *Vehicle System Dynamics* 13 (1984) 61–72.
[21] J.D. Robson, Road surface description and vehicle response, *International Journal of Vehicle Design* 1 (1979) 25–35.
[22] G. Ruf, The calculation of the vibrations of a four-wheeled vehicle, induced by random road roughness of the left and right track, *Vehicle System Dynamics* 7 (1978) 1–23.
[23] D. Cebon, E.D. Newland, The artificial generation of road surface topography by the inverse FFT method, *Proceeding of the Eighth IAVSD Symposium on Dynamics of Vehicles on Roads and on Railway Tracks*, Cambridge, MA, 1983, pp. 29–42.
[24] R.W. Rotenberg, *Vehicle Suspension*, Masinostrojenie, Moskou, 1972.
[25] A. Hac, Adaptive control of vehicle suspension, *Vehicle System Dynamics* 16 (1987) 57–74.